

Two carrier analysis of persistent photoconductivity in modulation-doped structures

S. E. Schacham,^{a)} R. A. Mena, E. J. Haugland, and S. A. Alterovitz
 NASA Lewis Research Center, Cleveland, Ohio 44135

(Received 6 September 1994; accepted for publication 2 March 1995)

A simultaneous fit of Hall and conductivity data gives quantitative results on the carrier concentration and mobility in both the quantum well and the parallel conduction channel. In this study this method was applied to reveal several new findings on the effect of persistent photoconductivity (PPC) on free-carrier concentrations and mobilities. The increase in the two-dimensional electron-gas (2DEG) concentration is significantly smaller than the apparent one derived from single carrier analysis of the Hall coefficient. In the two types of structures investigated, delta doped and continuously doped barrier, the apparent concentration almost doubles following illumination, while analysis reveals an increase of about 20% in the 2DEG. The effect of PPC on mobility depends on the structure. For the sample with a continuously doped barrier the mobility in the quantum well more than doubles. This increase is attributed to the effective screening of the ionized donors by the large electron concentration in the barrier. In the delta doped barrier sample the mobility is reduced by almost a factor of 2. This decrease is probably caused by strong coupling between the two wells, as is demonstrated by self-consistent analysis. © 1995 American Institute of Physics.

I. INTRODUCTION

The effect of persistent photoconductivity (PPC) has been observed in a large number of III-V and II-VI compounds, with various dopants, and different structures: bulk, heterojunctions, modulation-doped, or delta doped layers.¹⁻²⁵ It is manifested by the fact that photoexcited carriers do not recombine once the radiation is turned off, i.e., the excess carrier lifetime is extremely long, hours or even days, as long as the sample is maintained at low temperatures, typically below 150 K.^{10,24,25} In some systems, e.g., GaInP/InP or GaInP/GaAs, the effect was observed even at room temperature.^{2,14} The persistent increase in carrier concentration can be as large as four orders of magnitude.⁸

Persistent photoconductivity has been an issue of extensive experimental and theoretical interest, with most attention directed in recent years to heterostructures, in particular of AlGaAs/GaAs. Different observations and interpretations were presented by the various researchers. There seems to be a general consensus that at least two mechanisms are responsible for the effect.⁷⁻¹² The most common interpretation associates the phenomenon with photoexcitation of carriers from deep traps, with a microscopic barrier preventing immediate recombination. This process can be found in bulk material as well as in heterostructures. In the latter configuration a second mechanism is reported in which direct electron-hole generation followed by macroscopic separation gives rise to PPC. There are different reports as to the relative importance of each mechanism, as to the identification of the deep trap, and as to the source of persistence in each case.

It seems to be well accepted that the reason for the persistence of excess carriers generated from deep donors is due to separation in the k space. The deep traps are located away from the center of the Brillouin zone, either near the L or the X symmetry points. Once excited, the carriers relax rapidly to the Γ point, making recombination extremely difficult at low temperatures.¹⁻⁵ This mechanism, involving deep donors, was supported by the fact that in these structures the increase in concentration was accompanied by a decrease in mobility which was attributed to increased ionized scattering.⁴ Chand *et al.*, on the other hand, have studied over 50 samples of both n - and p -type AlGaAs, and since they consistently observed increase in mobilities they ruled out DX centers as the source for PPC in Si-doped AlGaAs.¹⁶ In a second paper they associated the persistence with the silicon dopant serving as a double acceptor which, by releasing an electron, changes its charge from -2 to -1 .¹⁷ The negative charge acts as a Coulomb barrier to electrons, thereby preventing recombination.

In heterojunctions PPC can originate by direct generation of electron-hole pairs and the lack of recombination is due to spatial separation between the original location of the electrons and their final destination.⁹⁻¹⁵ Such is the case in a modulation doped field effect transistor (MODFET) structure in which electrons generated at the barrier AlGaAs layer are transferred into the two-dimensional electron gas (2DEG) in the GaAs.¹⁰ In these structures the physical separation can also accompany the excitation of excess carriers from deep traps.^{7,10,18,19} While the increase in carrier concentration can be several orders of magnitude in bulk material, it is usually well below one order of magnitude in heterostructures.⁸

II. EXPERIMENT

Two MODFET structures, Q11 and Q12, were investigated and their schematics are shown in Fig. 1. The main

^{a)}National Research Council-NASA Senior Research Associate, on leave from the Department of Electrical Engineering and Solid State Institute, Technion-Israel Institute of Technology, Haifa 32000, Israel.

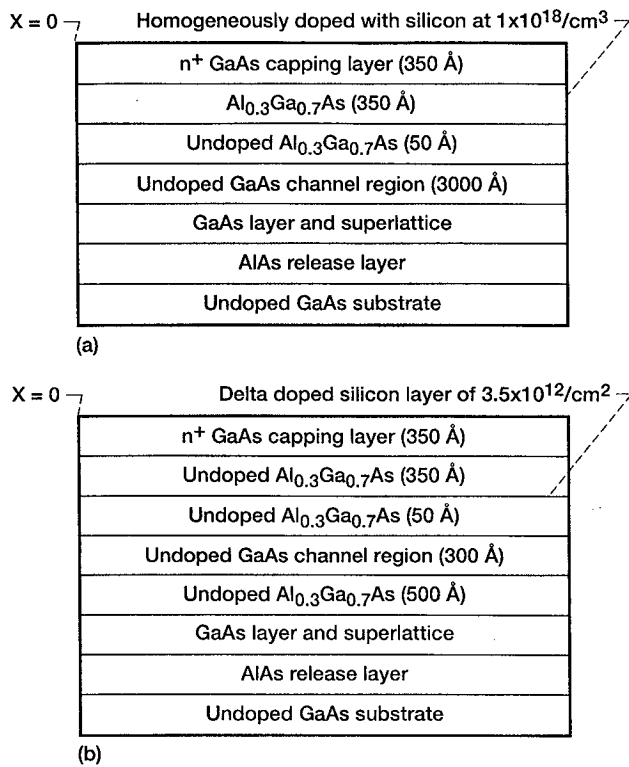


FIG. 1. Schematic cross section of MODFET structures with nominal dimensions (not to scale): (a) Q11 with continuously doped barrier and (b) Q12 with delta doped barrier.

difference between the two structures is that in the former the barrier was continuously doped, while in the latter the doping was applied via a delta layer in the barrier. All samples were grown in an MBE system, by QED Corporation. The layers were formed on a semi-insulating GaAs substrate, starting with an AlAs buffer, followed by a GaAs layer, and a superlattice buffer. All these were undoped. In structure Q11 the next layer was an undoped GaAs, 3000 Å wide, in which the well was formed. It was followed by an $\text{Al}_{0.30}\text{Ga}_{0.70}\text{As}$ barrier, composed of two parts: first the undoped spacer, nominally 50 Å wide, followed by a uniformly doped layer, nominally 350 Å wide, with a silicon concentration of $1 \times 10^{18} \text{ cm}^{-3}$. In structure Q12 the superlattice was followed by an undoped $\text{Al}_{0.30}\text{Ga}_{0.70}\text{As}$, 500 Å wide, then the undoped GaAs well, 300 Å wide. The $\text{Al}_{0.30}\text{Ga}_{0.70}\text{As}$ barrier was designed to be 400 Å wide, in which a Si delta doping was implemented with a sheet concentration of $3.5 \times 10^{12} \text{ cm}^{-2}$, placed 50 Å from the GaAs interface. In both structures the cap layer was n^+ GaAs with a donor concentration of over $3.5 \times 10^{18} \text{ cm}^{-3}$. The nominal thickness of the cap layer was 350 Å.

Both structures were analyzed by variable angle spectroscopic ellipsometry.²⁶ The results derived were significantly different from the nominal ones; in particular, the width of the barriers were found to be 270 Å in both samples rather than the nominal 400 Å. In all the simulations performed we used the layer thickness determined by ellipsometry. Since it is impossible to distinguish by ellipsometry between doped and undoped layers, one issue was left open, namely the thickness of the spacer. We assumed that the width of the

spacer remains as in the nominal specification, i.e., 50 Å, even though as a result the width of the doped AlGaAs layer in Q11 was reduced to 220 Å rather than the designed 350 Å.

The longitudinal voltage and the Hall voltage were recorded continuously as a function of the magnetic field up to the highest field accessible in our system, 1.4 T. This procedure was carried out for the samples in the dark from room temperature to 1.45 K. Then the samples were exposed to intense white light until the concentrations saturated. The window was covered, and the same measurements were performed starting from 1.45 K back to room temperature. For both structures the apparent concentrations and Hall mobility μ_H , as derived from the single carrier analysis of the Hall coefficient, were constant at lower temperatures. With increasing temperature (T) the concentration increased exponentially (Fig. 2), while the mobility dropped with μ_H proportional to T^{-2} (Fig. 3). The effect of PPC was to increase the apparent concentration at low temperatures by roughly 50%, from 6.2×10^{11} to $9.4 \times 10^{11} \text{ cm}^{-2}$ for sample Q11 and from 1.1×10^{12} to $1.7 \times 10^{12} \text{ cm}^{-2}$ for sample Q12. However, the effect of PPC on the mobility differed for the two samples. While the low-temperature Hall mobility for structure Q11 increased following illumination from 10^5 to $1.6 \times 10^5 \text{ cm}^2/\text{V s}$, for structure Q12 this mobility was lowered by PPC from 7.1×10^4 to $3.6 \times 10^4 \text{ cm}^2/\text{V s}$.

Finally, Shubnikov-de Haas (SdH) data was recorded on both samples, as a function of the perpendicular magnetic field up to 1.4 T at liquid-helium temperatures. The wave form as a function of inverse magnetic field renders an excellent quantitative, 2D selective estimate of the carrier concentration, as it is derived from the frequency of oscillations. The quantum relaxation time is obtained from the decay of the oscillation amplitude versus the magnetic field at a constant temperature. The derived carrier concentrations were 4.8×10^{11} in the dark and $7.5 \times 10^{11} \text{ cm}^{-2}$ after PPC for sample Q11, and 9.5×10^{11} and $1.3 \times 10^{12} \text{ cm}^{-2}$ after illumination for sample Q12. It should be mentioned that all oscillatory wave forms and subsequent fast Fourier-transform analysis show a single frequency, indicating contribution of a single carrier type to the pattern. This is in spite of the fact that the concentrations were larger than the typical threshold for population of the second sub-band. For both structures the relaxation time increased due to PPC, from 5×10^{-13} to $7 \times 10^{-13} \text{ s}$ for sample Q11, and from approximately 3×10^{-13} to $5 \times 10^{-13} \text{ s}$ for sample Q12. These latter calculations were performed at different temperatures with significant scatter in the results. However, the general trend of roughly a 50% increase was well established. A similar increase in the relaxation time due to PPC was reported by Fang *et al.*²⁷

III. THEORY AND ANALYSIS

Hall experiment is the conventional method for determination of carrier concentrations. Data reported in the literature for measurements performed in the dark on quantum structures frequently indicate an apparent increase in 2DEG carrier concentration as the temperature rises above approximately 150 K.^{15,24,25,28-30} This exponential increase was at

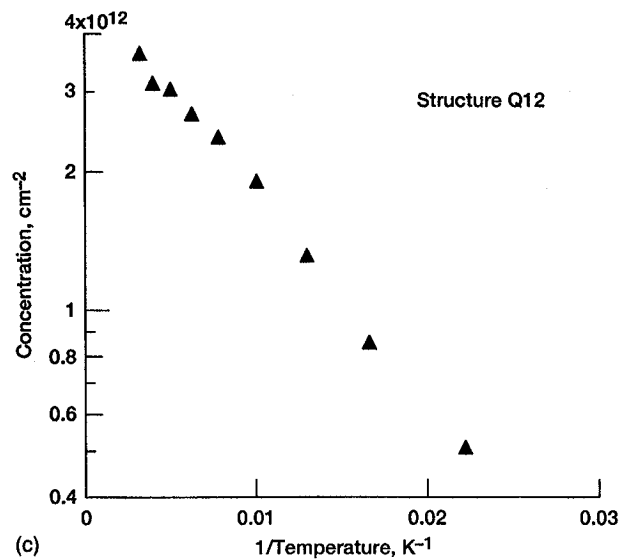
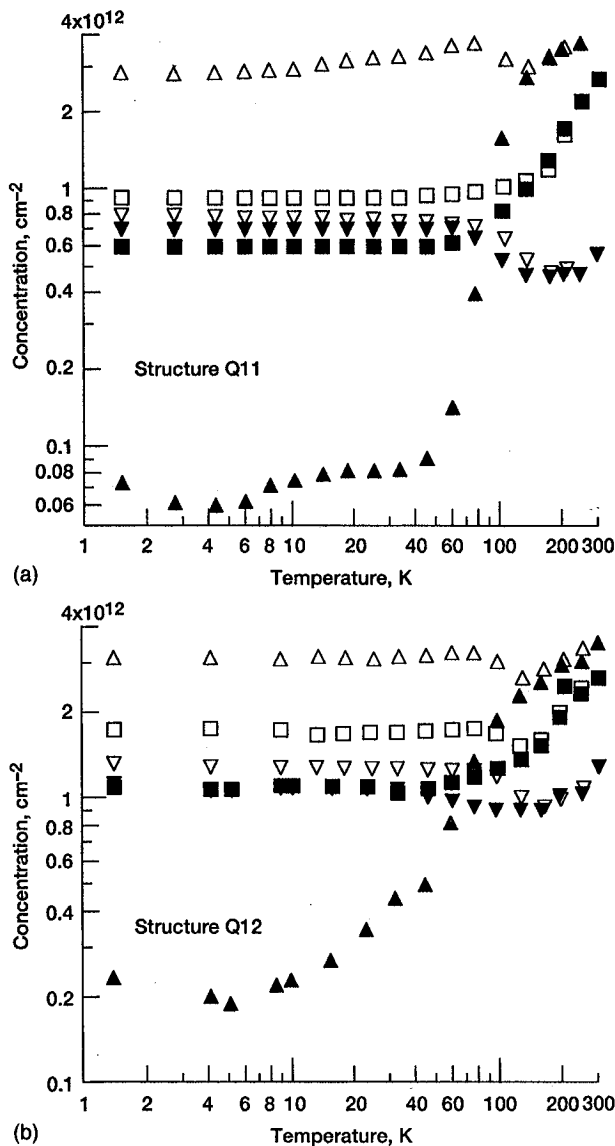


FIG. 2. Carrier concentrations vs temperature in dark and with PPC: Hall data (■, □), and derived from fitting [2DEG (▼, ▽) and parallel (▲, △)] concentrations. (a) For Q11, (b) for Q12. (c) Parallel carrier concentration vs inverse temperature in dark for Q12, showing freeze-out with activation energy of 10 or 20 meV.

tributed to an activation of the electrons out of the *DX* centers.²⁹ The Hall mobility of the 2D electrons also starts with a plateau. As the temperature is increased above roughly 100 K, the mobility drops approximately as T^{-2} .^{15,24,25,28-31} This decrease is attributed to scattering by polar optical phonons.^{24,31}

The data quoted above were derived directly from Hall and conductivity measurements; i.e., the carrier concentrations were assumed to be r/eR_H where R_H is the Hall coefficient while the mobility was obtained from the product $\mu_H = R_H \sigma$ where σ is the conductivity. The only correction applied at times was the introduction of a value different from 1 to the Hall scattering coefficient r .²⁹ In our analysis we assumed $r = 1$.

In most quantum structures more than a single type of carrier takes part in the transport. For example, in a MODFET structure three layers may play a role in the conductive process, namely the undoped well, the doped barrier, and the highly doped cap layer. The picture may be further complicated when more than one sub-band in the well is occupied.

As a result, the Hall concentration and mobility data are complex averages of the concentrations and mobilities of the constituent components.

An elegant way of handling the experimental data is by simultaneously fitting the longitudinal and transverse resistivities as function of magnetic field. Using this technique we were recently able to show that the 2DEG concentration in MODFET structures implemented in GaAs/AlGaAs remains unchanged from cryogenic to room temperatures.³⁰ The method was confirmed by comparing the low-temperature data to that obtained from SdH measurements. A similar procedure was later performed by Look *et al.*³² who arrived to the same conclusions. We use this method to analyze the temperature dependence of carrier concentrations and mobilities in quantum structures in the dark and in the presence of persistent photocarriers.

The experimental data is analyzed assuming that two carriers are taking part in the conduction process. Under such circumstances the longitudinal and transverse resistivities in

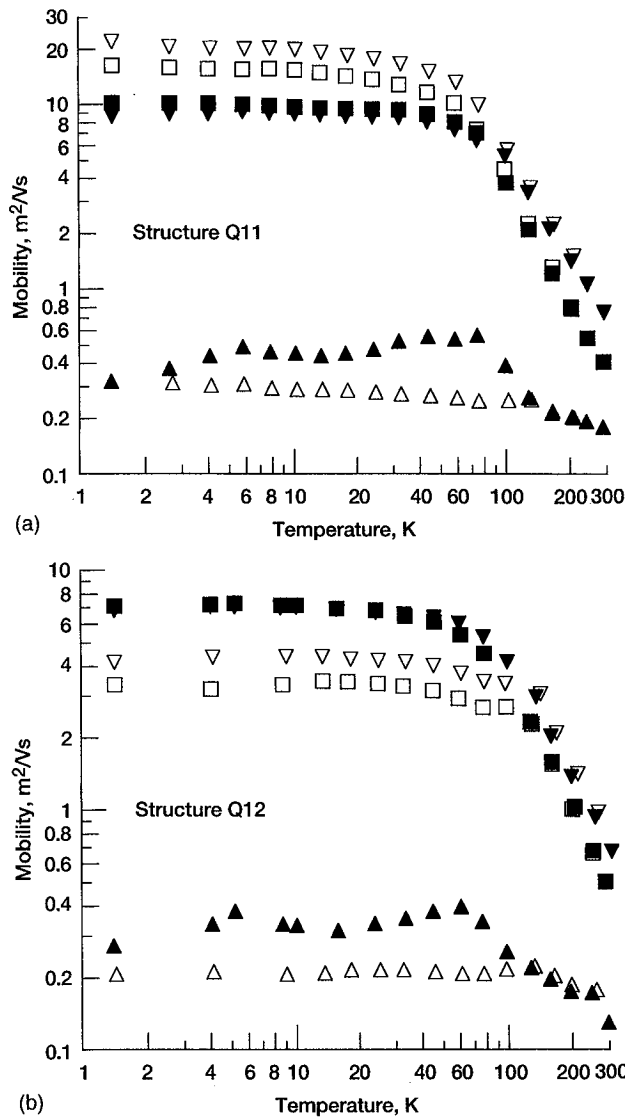


FIG. 3. Carrier mobility vs temperature in dark and with PPC: (a) for $Q11$, (b) for $Q12$. Same notation as in Fig. 2.

the presence of a perpendicular magnetic field B are given by³³

$$\rho_{xx} = E_x / J_x = D_{12} / (D_{12}^2 + A_{12}^2), \quad (1)$$

$$\rho_{xy} = E_y / J_x = R_H B = A_{12} / (D_{12}^2 + A_{12}^2), \quad (2)$$

with the coefficients defined by $D_i = n_i e^2 \tau_i / m_i^*$ ($1 + \omega_{ci}^2 \tau_i^2$), $A_i = \omega_{ci} \tau_i D_i$, $D_{12} = D_1 + D_2$, and $A_{12} = A_1 + A_2$. The two carriers, indicated by the index i , have concentrations n_i , effective masses m_i^* , and scattering times τ_i . The electric field is E while the longitudinal current density is denoted by J_x . The Hall scattering factor is assumed to be 1. The magnetic-field dependence is introduced through the cyclotron frequency $\omega_c = eB/m^*$.

This method can be extended to more than two carriers. However, the additional carriers should have a large enough effect on the resistivities for the multicarrier analysis to converge. With the data reported in this work a three carrier analysis failed, indicating that if a third carrier is involved in the conduction process, either its mobility is very close to

one of the other two, or its concentration is too low to be noticed. This latter assumption agrees with the absence of superposition in the SdH wave form.

The procedure we employed in order to analyze the experimental data was to fit simultaneously the longitudinal and transverse voltages as a function of magnetic field, using a nonlinear least-square fit with Eqs. (1) and (2). Four parameters are derived, namely the two concentrations n_1 and n_2 , and the two mobilities μ_1 and μ_2 ($\mu = e\tau/m^*$). At lower temperatures the separation of these parameters gets less accurate as the contribution of the parallel carrier to the conductivity get relatively smaller. However, our method enabled the derivation of all four parameters with high accuracy, to temperatures as low as 10 K.³⁰ This straightforward approach seems to give better results than the method of employing intermediate parameters.³² This latter method seems to limit the temperature range of its applicability to much higher temperatures. In some structures only the product of mobility and concentration was attainable even at room temperature.³²

In addition, self-consistent analysis of the structures was performed. The analysis is based on a numerical solution of Schrodinger and Poisson equations simultaneously in all the different layers, taking into account the appropriate boundary conditions. The solution provides the energy-band structures, the carrier concentrations, the confined energy levels, along with the respective wave functions. The pre-PPC conditions were analyzed allowing for carrier freeze-out. However, the program cannot handle persistent conductivity, since one has to introduce two donors: deep donors (DX) which, once ionized, do not recombine, and the shallow Si donors which go through freeze-out. Moreover, permanent excess carriers can be produced by direct electron-hole generation followed by macroscopic separation. To simulate the effect of PPC we performed the self-consistent analysis forcing full ionization of all dopants. The second drawback of this simulation is that the only dopant introduced in the barrier was the shallow one. No deep centers (DX centers) were included. This simulation is used mostly for qualitative understanding of the PPC process. The quantitative implications are limited, in particular for the barrier. All simulations were performed for liquid-helium temperatures.

IV. RESULTS AND DISCUSSION

Figure 2(a) shows the carrier concentrations before and after illumination for sample $Q11$ while Fig. 2(b) shows the same for sample $Q12$. Each figure includes the Hall data and the result of the magnetic-field dependent analysis providing the 2DEG and the parallel concentrations. Prior to illumination the 2DEG population remains constant, while that of the parallel layer decreases exponentially with the inverse temperature. One of the surprising findings of the present analysis is the small effect of persistent photoconductivity on the two-dimensional concentration. The figures demonstrate very clearly that there is a very little increase in the 2DEG concentration as a result of the illumination. For example, at 10 K the increase is from 7.0×10^{11} to $7.8 \times 10^{11} \text{ cm}^{-2}$ for sample $Q11$ and from 1.1×10^{12} to $1.3 \times 10^{12} \text{ cm}^{-2}$ for sample $Q12$, much below the apparent increase of the Hall

concentration. In both cases the PPC concentrations agree extremely well with the values derived from the SdH analysis (7.5×10^{11} and $1.3 \times 10^{12} \text{ cm}^{-2}$, respectively), but less well for the concentrations prior to illumination, in particular for the *Q11* structure. The reason is twofold. First, the accuracy of fitting process improves if the conductivities of the two contributing layers are of similar magnitude. Thus with no PPC the accuracy of the derived second carrier concentration is limited as its conductivity is much smaller than that of the 2DEG, due to its small concentration and mobility. Second, as discussed below, the unconfined structure of sample *Q11* on its substrate side results in extended states which cannot be considered 2D and therefore will not be observed in the SdH analysis.

The effect of PPC is much more significant on the carrier concentrations in the parallel layer. Following illumination the low-temperature concentrations increased by more than an order of magnitude, from 6×10^{10} to $3 \times 10^{12} \text{ cm}^{-2}$ in structure *Q11* and from 2×10^{11} to $3 \times 10^{12} \text{ cm}^{-2}$ in structure *Q12*. Interestingly, this concentration is almost temperature independent, very much like the 2DEG concentration, only 3–4 times larger. Unlike the previous case, the accuracy of the fitting process in this region is very high, due to the large concentrations in the parallel layer.

The fundamental question is where the location of this second parallel free carrier is. In a previous work it was claimed that these are electrons in the highly doped cap layer.³² The argument was based on the fact that the conductivity of the layer remains unchanged as the temperature was lowered, typical for degenerate material. This is not the case in our structures. In Fig. 2(c) we show the carrier concentration in the parallel layer of sample *Q12* prior to illumination for $T > 40 \text{ K}$. From the logarithm of the concentration versus $1/T$ the activation energy can be derived. Depending on whether compensation is absent or present, a factor of 2 in the slope has to be included. Thus the derived ionization energy is about 20 meV if no compensation is assumed, or 10 meV otherwise. Even if the cap layer electrons were not degenerate, the activation energy of silicon in GaAs is 5.8 meV. The value of an activation energy of 10 or 20 meV rules out the possibility of the second carrier being electrons in the GaAs cap layer. On the other hand, these energy values are within the range of Si as a shallow donor in AlGaAs.¹⁷ Thus the clear freeze-out of carriers all the way down to 20 K indicates that in our structures the second carrier derived from the analysis is not in the cap layer, but rather in the AlGaAs barrier. Only at the lowest temperatures (below 20 K for *Q12* and below 40 K for *Q11*) does the concentration level off. Here it is most likely that a different carrier with similar mobility, probably electrons in the cap layer, may dominate. However, after illumination the electrons accumulated in the AlGaAs are degenerate, as manifested by their constant concentration and mobility.

Figures 3(a) and 3(b) shows the mobilities in both samples, in the dark and after illumination. The mobility in the parallel conduction channel is low and fairly constant. The PPC results in a slight decrease of this mobility, with the final mobility being even less temperature dependent than the original one. The marked difference between the two

samples is in the two-dimensional mobility at its plateau (below 100 K). Before illumination these mobilities are quite similar for both structures, namely $92\,000 \text{ cm}^2/\text{V s}$ for sample *Q11* and $74\,000 \text{ cm}^2/\text{V s}$ for sample *Q12*. However, the effect of PPC on the two structures is dramatically different. While the mobility more than doubles for *Q11*, reaching about $200\,000 \text{ cm}^2/\text{V s}$ after illumination, it drops by almost the same factor for *Q12* due to PPC, to $44\,000 \text{ cm}^2/\text{V s}$. Thus it is obvious that the location of the doping in the barrier has a dramatic consequence on the effect of PPC on carrier mobility. For both structures the change in mobility is extremely large, considering an increase in 2DEG concentration of around 20%.

A steep increase in mobility with carrier concentration was reported by Higgins *et al.*³⁴ They observed an increase with concentration to the power of 3.5–4.5, rather than the power of 1–1.5 reported by others.³⁵ They performed their experiments on samples in which the undoped spacers (150–200 Å) are wider than the narrow supply layer (100 Å, with dopant concentration of 10^{18} cm^{-3}), in AlGaAs with an Al fraction of only 0.23–0.24. The maximum 2DEG concentration they attained after illumination was only $2.5 \times 10^{11} \text{ cm}^{-2}$. Their interpretation attributed the large change in mobility to discharging of acceptors in the spacer (with an estimated concentration of at least 10^{17} cm^{-3}). A similar steep mobility dependence was reported by Kastalsky and Hwang,¹⁰ again in a sample with a wide spacer (190 Å). They compared similar structures with different spacer widths and found out that the narrower the spacer, the slower the increase in mobility with concentration. With a spacer of only 20 Å the mobility increases first roughly linearly with concentration and after increasing by about 15% it started decreasing linearly by some 25% till the concentration saturated. The authors excluded intersub-band scattering as a source of this drop since it was not abrupt enough and the mobility never started increasing again as it should with this type of scattering. Their explanation of their findings was based on two processes. First, as more carriers are generated, the Fermi level (E_F) rises and as a result the Coulomb scattering is reduced. However, once electrons start accumulating in the barrier the Fermi level stops rising. With continued excitation more donors are ionized, resulting in a dropping mobility. They claim that the excess carriers are generated both from DX centers in the barrier and from macroscopic charge separation following electron-hole generation in the well. A steep increase in mobility was also reported by Rorison *et al.*³⁶ They associated this increase with localized electrons which are due to potential fluctuations in the 2DEG. However, this effect takes place only at much lower concentrations, of about $2 \times 10^{11} \text{ cm}^{-2}$, at which the carrier energy is smaller than the root-mean-square value of the fluctuations. This process cannot explain the increase in mobility at the carrier concentrations which we are dealing with in sample *Q11*, which are $4 \times$ larger than those of Rorison *et al.*

In the previous paragraph the increase in mobility was associated with the increase in 2DEG concentration. The dependence of the mobility only on the concentration of electrons in the GaAs well is misleading. Rather we tend to associate the large increase in mobility in sample *Q11* also

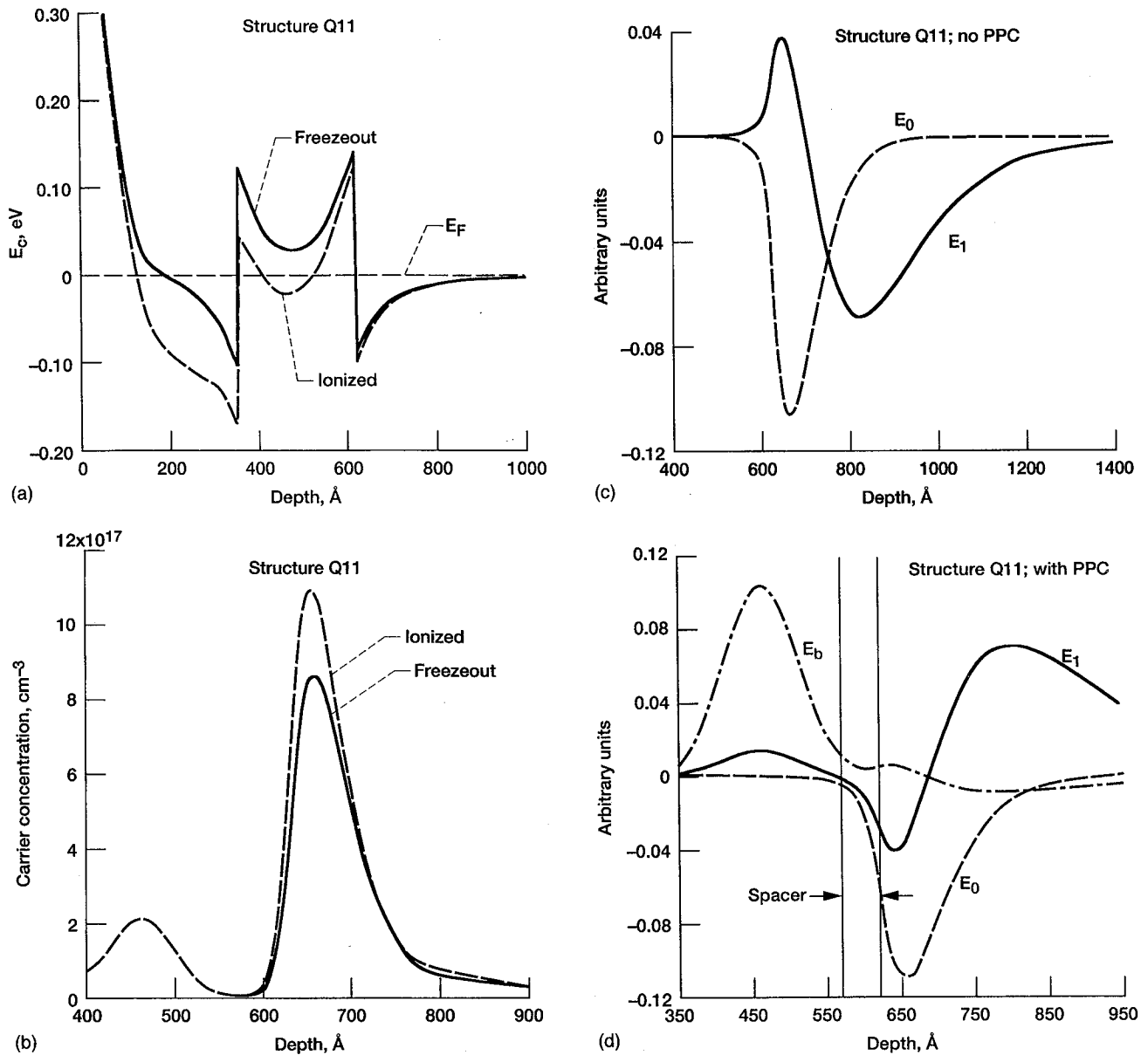


FIG. 4. Results of self-consistent simulation for Q11 in the dark (freeze-out) and with PPC (fully ionized): (a) conduction-band structure, (b) electron concentration profile, (c) wave functions of confined states, no PPC ($x=0$ at top contact, see Fig. 1), and (d) wave functions with PPC; spacer region is marked to show good confinement.

with the extreme increase in the electron concentration in the barrier. These carriers screen the ionized donors, thus improving the mobility further. Figure 4 shows the results of self-consistent simulation of the effect of PPC on the carrier concentration in the barrier. The figure shows the band bending assuming all carriers are ionized (PPC), as compared to freeze-out conditions (dark). Also shown is the carrier profile. The increased electron population is evident throughout the barrier, including at the edge of the spacer layer. In this area the most effective scatterers are present, being in closest proximity to the 2DEG. Therefore the most effective screening is achieved by a relatively small amount of excess electrons located in this region.

The concentrations calculated from the self-consistent analysis for the 2DEG in Q11, $8.24 \times 10^{11} \text{ cm}^{-2}$ with freeze-out and $9.94 \times 10^{11} \text{ cm}^{-2}$ when fully ionized, are in good

agreement with the measured ones. On the other hand, the concentration calculated for the barrier assuming full ionization is much smaller than the experimental concentration derived from the simultaneous fit for PPC conditions. As discussed before, the results derived from the simulation for the barrier cannot be taken quantitatively. The error may indicate that either the concentration of deep donors is larger than that of the shallow ones (the latter are used in the computation), or, alternatively, it is possible that the width of the doped region is larger than obtained from ellipsometry. However, simulations in which the supply layer was widened to its full nominal value did not result in a significant increase in the concentration of the barrier, while increasing the 2DEG concentration above the measured values.

Figure 4(c) and 4(d) shows the wave functions which correspond to two confined levels within the GaAs, at

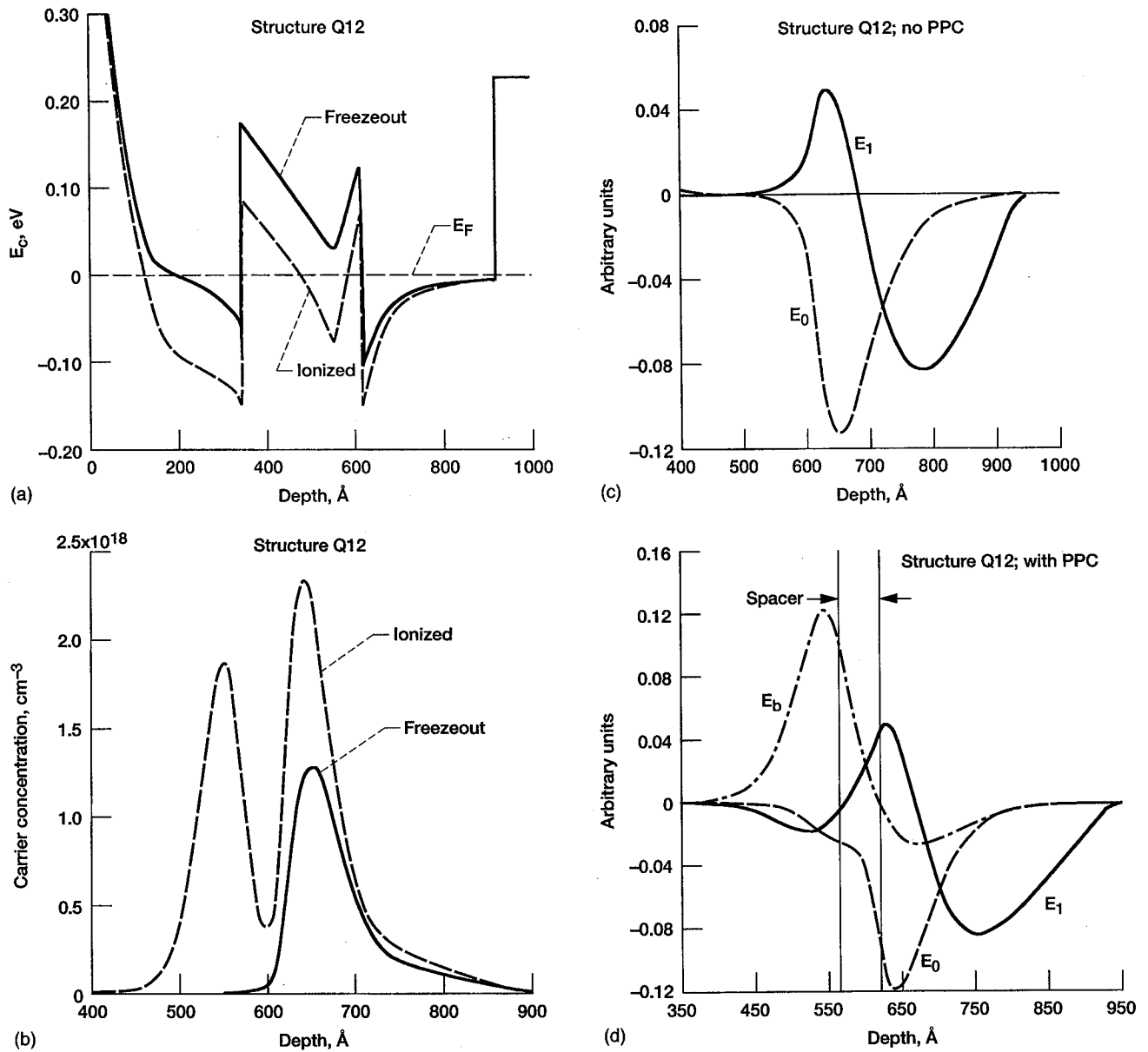


FIG. 5. Same as Fig. 4 for sample *Q12*. In (d) spacer region is marked to show the penetration of the wave function.

$E_0=31.5$ meV and $E_1=4.12$ meV below the Fermi level for fully ionized conditions, with a third level, $E_b=4.96$ meV below the E_F in the barrier. Similarly, under freeze-out the eigenvalues are $E_0=26.5$ meV and $E_1=3.1$ meV below the E_F in the GaAs (no confined level in the AlGaAs). The shallow level in *Q11* extends throughout the GaAs layer. Unlike *Q12*, here there is no second AlGaAs barrier. Thus electrons with a few millielectron volts below the Fermi level are more 3D than 2D carriers. Since the amplitude of the magnetoresistance oscillations produced by a 3D carrier is substantially lower than that produced by a 2D one, the oscillations generated by carriers in extended states are negligible in comparison with those produced by carriers at the bottom of the well. This gives an indication why the results of the SdH analysis, that estimates the 2D carriers only, render a concentration substantially lower than that derived from the Hall data or from the self-consistent simulation for this structure.

Why does the mobility of carriers in the 2DEG of structure *Q12* not increase with PPC in the same manner as in *Q11* but rather decreases? The most common reason for a mobility drop with increased carrier concentration is that the Fermi level reaches an excited sub-band, initiating intersub-band scattering. To examine this option we analyzed the confined energy levels for this structure. Assuming carrier freeze-out, two energy sub-bands are confined to the well, at $E_0=35.5$ meV and $E_1=4.94$ meV below the E_F . Thus two sub-bands must be occupied even in the dark. The spacing between these sub-bands corresponds to a concentration of 8.6×10^{11} cm $^{-2}$. In the fully ionized simulation there are again two confined states in the GaAs well, located at $E_0=54.4$ meV and $E_1=9.56$ meV below E_F . The calculated 2DEG concentration in the dark, 1.15×10^{12} cm $^{-2}$, is close to the measured one. With PPC, the calculated value of 1.69×10^{12} cm $^{-2}$ is 25% higher than the measured concen-

tration. The larger inaccuracy in this case is not surprising since the PPC is simulated by assuming all the donors in the delta doping are ionized. Since in this case the confined energy level within the barrier is much below the Fermi level, i.e., $E_b = 31.1$ meV below E_F , it pushes the confined levels of the 2DEG further down, resulting in an artificially high calculated value for its concentration. Thus the self-consistent analysis shows that there are two occupied sub-bands in the 2DEG well before and after illumination. Hence the sudden drop in mobility observed following illumination cannot be attributed to a new intersub-band scattering, since two sub-bands were occupied before illumination.

The drop in the mobility in *Q12* is due to the coupling between the GaAs well and the AlGaAs supply layer. In these type of structures there are two triangular wells³⁷ due to the conduction-band discontinuity. One in the undoped GaAs layer, in which the 2DEG high mobility transport takes place, the other is in the AlGaAs barrier, generated by the delta doping. Figure 5 presents the results of the self-consistent computations on this structure. It shows the wave functions of the different confined states assuming full ionization or freeze-out. The wave functions shown are significantly different from those of Fig. 4. While in *Q11* the wave function of the deeper bound state is limited to the well, this wave function in *Q12* extends well into the barrier, past its delta doped layer. This result is in spite of the fact the respective energies are 54.4 meV below E_F in *Q12* while it is only 31.5 meV below E_F in *Q11*. Since the mobility in the barrier is almost two orders of magnitude lower than that reached in the well, this coupling results in a substantial reduction in the mobility of electrons in the 2D gas of *Q12*.

The last piece of data which has to be explained is the increase in the quantum relaxation time for structure *Q12* in spite of the decreased mobility. The ratio between the classical scattering time and quantum relaxation time decreases from 9.3 to 3.4 following illumination. The various mechanisms dictating this ratio are discussed by Das Sarma and Stern.³⁸ The basic difference between the two times is that mobility is hardly affected by small-angle scattering, since the associated classical time has a $(1 - \cos \theta)$ weighing factor, while quantum relaxation is affected equally by all scatterers. Thus the quantum time depends on the total number of scatterers, on their "quantity," whereas the classical time depends on their "quality." Therefore the more isotropic is the scattering, the more similar the two and the smaller the ratio. Three parameters determine how isotropic is the process, namely the distance between the scatterers and the electron plane, z_i , the Fermi wave vector k_F , and the screening parameter q_{TF} .^{27,38} The wave vector in 2D is given by $k_F = (2\pi N_s/g_v)^{1/2}$ where N_s is the 2D electron concentration and g_v is the degeneracy (1 for GaAs, 2 for Si). For a 2D concentration of 10^{12} cm⁻², $k_F = 2.5 \times 10^6$ cm⁻¹ in GaAs and 1.8×10^6 cm⁻¹ in Si. The screening parameter is given by $q_{TF} = 2g_v m^* e^2 / \kappa \hbar^2$, where κ is the dielectric constant. This parameter is equal to 2×10^6 cm⁻¹ for GaAs and to 1.9×10^7 cm⁻¹ for Si.³⁸ The ratio between the times increases with increasing k_F/q_{TF} (which explains the ratio of 1 in Si^{27,38}), and with the product $z_i \cdot q_{TF}$.³⁸ For our structures the spacer is 50 Å wide; thus this product is equal 1. For k_F/q_{TF} equal

also to 1, the ratio between the scattering times is about 9. This agrees well with our result prior to illumination. The effect of PPC is twofold: on one hand, the large increase in free-carrier concentration in the barrier and the increased 2DEG concentration improve the screening of the remote ionized centers, as is the case in *Q11*. This results in a longer quantum relaxation time in both samples. However, these centers have little influence on the mobility as compared with that of the centers in close proximity to the interface. The self-consistent analysis of structure *Q12* indicates that the 2DEG penetrates into the barrier, greatly increasing the destructive role of the centers associated with the Si delta layer. This can be interpreted as effectively reducing the width of the spacer. An effective spacer width of 20 Å will result in the measured ratio of 3.

V. CONCLUSIONS

The separation between the concentrations and mobilities of electrons in the 2DEG and in the parallel layer reveal interesting findings on the effect of PPC on MODFET structures. First, the increase in carrier concentration in the 2DEG is much smaller than appears from the Hall measurement. The apparent increase in the Hall concentration is almost entirely due to the large increase in the parallel layer carrier concentration. Our analysis indicates that the parallel layer carriers are electrons in the AlGaAs barrier. These carriers go through freeze-out in the dark, with an activation of energy 10 or 20 meV, while with PPC their concentrations remains unchanged, being roughly equal to 3×10^{12} cm⁻².

The effect of PPC on mobility depends extensively on the location and distribution of the dopant. While with a continuously doped barrier the mobility more than doubled following illumination, it fell to half its original value in the sample in which the dopant was introduced as a delta layer in the AlGaAs. With the aid of self-consistent analysis we have shown that the increase in the first case is mostly due to the effective screening of the ionized donors by the large concentration of electrons in the continuously doped barrier. On the other hand, the band bending between the two wells formed by the delta doping results in strong coupling between the layers. As a result, the 2DEG electrons are not completely confined to the GaAs well, but penetrate into the barrier. This results in a drastic drop in their mobility. The self-consistent analysis should be improved to simulate real life PPC and to include the distribution in energy of *DX* centers with their extremely long recombination time, in order to obtain more quantitative results. However, we believe that the qualitative conclusions we derived from the self-consistent analysis are due to first-order effects and will not change when these refinements in the calculations will be included.

ACKNOWLEDGMENT

The authors acknowledge the expertise of QED for preparing the MBE structures.

¹J. Y. Lin, A. Dissanayake, G. Brown, and H. X. Jiang, Phys. Rev. B **42**, 5855 (1990).

²S. Ben Amor, L. Dmowski, J. C. Portal, N. J. Pulsford, R. J. Nicolas, J.

- Singleton, and M. Razeghi, *J. Appl. Phys.* **65**, 2756 (1989).
- ³D. V. Lang and R. A. Logan, *Phys. Rev. Lett.* **39**, 635 (1977).
- ⁴D. V. Lang, R. A. Logan, and M. Joros, *Phys. Rev. B* **19**, 1015 (1979).
- ⁵D. K. Maude, J. C. Portal, L. Dmowski, T. Foster, L. Eaves, M. Nathan, M. Heiblum, J. J. Harris, and R. B. Beall, *Phys. Rev. Lett.* **59**, 815 (1987).
- ⁶S. Arscott, M. Missous, and L. Dobaczewski, *Semicond. Sci. Technol.* **7**, 620 (1992).
- ⁷R. Fletcher, E. Zaremba, M. D'Iorio, C. T. Foxon, and J. J. Harris, *Phys. Rev. B* **41**, 10649 (1990).
- ⁸D. E. Lacklison, J. J. Harris, C. T. Foxon, J. Hewett, D. Hilton, and C. Roberts, *Semicond. Sci. Technol.* **3**, 633 (1988).
- ⁹T. N. Theis and S. L. Wright, *Appl. Phys. Lett.* **48**, 1374 (1986).
- ¹⁰A. Kastalsky and J. C. M. Hwang, *Solid State Commun.* **51**, 317 (1984).
- ¹¹E. F. Schubert, A. Fischer, and K. Ploog, *Solid State Electron.* **29**, 173 (1986).
- ¹²E. F. Schubert, A. Fischer, and K. Ploog, *Phys. Rev. B* **31**, 7937 (1985).
- ¹³H. J. Queisser and D. E. Theodorou, *Phys. Rev. Lett.* **43**, 401 (1979).
- ¹⁴Y.-G. Zhao, G. Zhao, J. L. Brebner, A. Bensaada, and R. A. Masut, *Semicond. Sci. Technol.* **7**, 1359 (1992).
- ¹⁵D. M. Collins, D. E. Mars, B. Fischer, and C. Kocot, *J. Appl. Phys.* **54**, 857 (1983).
- ¹⁶N. Chand, R. Fischer, J. Klem, T. Henderson, P. Pearah, W. T. Masselnik, Y. C. Chang, and H. Morkoc, *J. Vac. Sci. Technol. B* **3**, 644 (1985).
- ¹⁷N. Chand, T. Henderson, J. Klem, W. T. Masselnik, R. Fischer, Y. C. Chang, and H. Morkoc, *Phys. Rev. B* **30**, 4481 (1984).
- ¹⁸J. Klem, W. T. Masselnik, D. Arnold, R. Fischer, T. J. Drummond, H. Morkoc, K. Lee, and M. S. Shur, *J. Appl. Phys.* **54**, 5214 (1983).
- ¹⁹J. Shen, S. Tehrani, H. Goronkin, R. Droopad, and G. Maracas, *J. Appl. Phys.* **71**, 5985 (1992).
- ²⁰M. I. Nathan, M. Heiblum, J. Klem, and H. Morkoc, *J. Vac. Sci. Technol. B* **2**, 167 (1984).
- ²¹H. L. Stormer, A. C. Gossard, W. Wiegmann, R. Blondel, and K. Baldwin, *Appl. Phys. Lett.* **44**, 139 (1984).
- ²²K. Kitahara, M. Oshino, and M. Ozeki, *Jpn. J. Appl. Phys.* **27**, L110 (1988).
- ²³H. P. Hjalmarson and T. J. Drummond, *Appl. Phys. Lett.* **48**, 656 (1986).
- ²⁴E. F. Schubert, A. Fischer, and K. Ploog, *Appl. Phys. A* **33**, 63 (1984).
- ²⁵E. E. Mendez, P. J. Price, and M. Heiblum, *Appl. Phys. Lett.* **45**, 294 (1985).
- ²⁶S. A. Alterovitz, P. G. Snyder, K. G. Merkel, J. A. Woollam, D. C. Randlescu, and L. F. Eastman, *J. Appl. Phys.* **63**, 5081 (1988).
- ²⁷F. F. Fang, T. P. Smith, and S. L. Wright, *Surf. Sci.* **196**, 310 (1987).
- ²⁸Y. Horikoshi, A. Fischer, E. F. Schubert, and K. Ploog, *Jpn. J. Appl. Phys.* **26**, 263 (1987).
- ²⁹K. Bhattacharyya, J. O. Orwa, and S. M. Goodnick, *J. Appl. Phys.* **73**, 4396 (1993).
- ³⁰S. E. Schacham, R. A. Mena, E. J. Haugland, and S. A. Alterovitz, *Appl. Phys. Lett.* **62**, 1283 (1993).
- ³¹K. Lee, M. S. Shur, T. J. Drummond, and H. Morkoc, *J. Appl. Phys.* **54**, 6432 (1983).
- ³²D. C. Look, C. E. Stutz, and C. A. Bozada, *J. Appl. Phys.* **74**, 311 (1993).
- ³³M. J. Kane, N. Apsley, D. A. Anderson, L. L. Taylor, and T. Kerr, *J. Phys. C* **18**, 5629 (1985).
- ³⁴R. J. Higgins, K. P. Martin, D. A. Syphers, J. A. Van Vechten, and S. C. Palmateer, *Phys. Rev. B* **35**, 2707 (1987).
- ³⁵H. L. Stormer, A. C. Gossard, W. Wiegmann, and K. Baldwin, *Appl. Phys. Lett.* **39**, 913 (1981).
- ³⁶J. M. Rorison, M. J. Kane, D. C. Herbert, M. S. Skolnick, L. L. Taylor, and S. J. Bass, *Semicond. Sci. Technol.* **3**, 12 (1988).
- ³⁷B. Jogai, P. W. Yu, and D. C. Streit, *J. Appl. Phys.* **75**, 1586 (1994).
- ³⁸S. Das Sarma and F. Stern, *Phys. Rev. B* **32**, 8442 (1985).

